STABILITY AND FAILURE BEHAVIOUR OF THE VAIONT SLIDE

Oldrich HUNGR & Jordan AARON

University of British Columbia, 6330 Stores Rd., Vancouver, B.C., V6T 1Z4, Canada

ABSTRACT

The statics and dynamics of the Vaiont Slide have been studied using several models based on the theory of Limit Equilibrium, in two and three dimensions. The analyses confirmed the need to consider low bedding-parallel strength of much of the rupture surface, combined with high piezometric pressures. The role of internal strength of the rock mass is also important, to a degree that depends on the mobilization of rock mass cohesion. The slide was asymmetric and laterally constrained and is likely to have detached in two stages, separated by a surface under diagonal tension. A displacement wave analysis indicates that the slide velocity is unlikely to have exceeded 10 m/s.

KEY WORDS: *Landslide, rock slide, limit equilibrium analysis, dynamic analysis, displacement wave*

INTRODUCTION

The Vaiont rock slide of October 9, 1963 was the second deadliest single landslide event in European history. It is further remarkable in that both the landslide itself and the disastrous displacement wave which caused more than 2000 fatalities, were the result of the artificial impoundment of a reservoir. Even more important for geologists and engineers is the fact that the full extent of the landslide was recognized, investigated, measured, monitored and predicted by knowledgeable professionals right up to the moment of failure. What was not anticipated, however, was the catastrophic speed with which the failure scenario unfolded. No-one expected the gigantic, sudden release of energy, which produced a wave overtopping the Vaiont dam by a height of 140 m and sent a deadly surge of water towards the town of Longarone in the Piave Valley.

The Vaiont Slide has been the subject of a fair amount of investigation and data gathering both before and after 1963 and a very large number of publications. However, due to the large scale of the event, its timing in the nineteen-sixties and economic circumstances, the factual data base is still quite limited, compared to data sets commonly available for contemporary mining and civil geotechnical slope problems. This makes quantitative analyses very difficult. The recently-acquired Lidar topography and detailed structural analyses compiled by SUPERCHI (2012) are a significant addition to the data base.

The purpose of this invited paper is to attempt a simple three-dimensional analysis of the mechanism of failure and propagation of the landslide, based on a summary of existing data. Specifically, the goal is to attempt a fresh reconstruction of the sliding surface and examine its stability and dynamics using best estimates of material properties and piezometric conditions. The instability of the north slope of Mt. Toc is not difficult to explain. The primary focus of this analysis is the failure behaviour. Why was energy released so suddenly and why did the enormous mass of rock and soil move so rapidly and cover such a large distance? What was the mechanism of interaction with the water stored in the reservoir?

51

PREVIOUS ANALYSES

Detailed original studies of the Vaiont reservoir slopes were made by geologists, as summarized by SEMENZA & GHIROTTI (2000). These studies, supported by extensive field mapping and limited drilling site investigations, produced a reliable trace of the surface outline of the sliding mass, a series of interpolated cross-sections and proof that a large part of the sliding surface follows a bedding-parallel zone, pre-sheared by a pre-historic landslide of similar geometry. This data, supplemented with additional fieldwork, was used in a comprehensive engineering analysis of the event by Hendron & Patton (1985). The latter authors carried out approximate analysis of slope stability in 2 and 3 dimensions, as well as a two-dimensional analysis of landslide motion. Influenced by earlier ideas by MENCL (1966), VOIGHT & FAUST (1982) and others, they contributed the following key findings:

The major part of the Vaiont sliding surface followed clay-coated bedding planes in Late Jurassic limestone units, pre-sheared by the prehistoric landslide. Although the bentonitic clay fillings on the bedding planes had laboratory residual friction angles of 5° to 16°, the average value for the shear zone, accounting for some rock-to rock contact, was estimated as 10° to 12°.

Many of the downslope cross-sections had a listric compound shape resulting from the synclinal geometry of the calcareous strata (Erto Syncline), so that the sliding stability was influenced by the internal strength of the displaced rock, in order to make downslope motion kinematically feasible (MENCL, 1966, HUTCHINSON, 1988).

The bedding structure plunged to the west, so that the sliding surface had to pass through the limestone rock mass in order to daylight on the right (east) flank of the landslide.

There was high piezometric pressure within the unstable rock mass, caused by a combination of toe submergence by the reservoir and infiltration coinciding with heavy rainfalls preceding the event.

A substantial loss of strength of the sliding mass was required to enable the landslide to reach the observed total displacement and velocity. Hendron and Patton (in an analysis carried out by D. Anderson) assumed that strength loss occurred on the part of the sliding surface controlled by the bedding planes and that it was due to pore-pressure increase caused by heating (as proposed by VOIGHT & FAUST, 1982, see discussion below).

The authors consider most of these conclusions to be still largely valid at the present time.

Detailed structural analysis and a geomechanical characterization of the rock masses was conducted recently by a research group from the University of Padova (SUPERCHI 2012, SUPERCHI *et alii*, 2010). Its findings are that the limestone beds are folded not only in the north-sound trending syncline, but also in a less pronounced east-west trending (Messalezza) syncline. The two perpendicular superimposed folding episodes create oblique dips in the upper part of the sliding surface and small interference structures in the central part of the sliding surface. This research also advanced a hypothesis that the failure occurred in two closely-related stages.

RECONSTRUCTION OF THE SLIDING SURFACE

The rupture surface of the 1963 slide was reconstructed by the following means:

1) By accepting the three downslope sections drawn by D. Rossi and E. Semenza and reproduced by HENDRON & PATTON (1985) in their Fig. 15, 17 and 19. It is noted that these sections coincide well with the levels of the main sheared zones identified in a number of boreholes drilled in 1964, following the slide.

2) By ensuring that the downslope (toe) outline of the rupture surface coincides with the outcrop of a
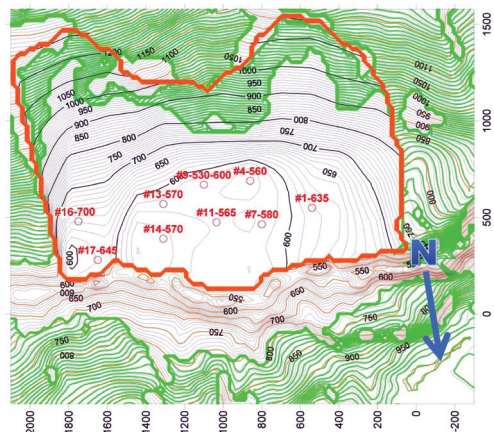
Fig. 1 - *Reconstructed rupture surface of the Vaiont Slide, related to the boundaries of the mesh used in the stability analyses. Boreholes with reported elevations of the main shear zone are shown. Dimensions in metres. The UTM coordinates of the origin lower right corner of the map (-300,-500 are 2313965,5127994) and the azimuth of the vertical axis is 190º*

"tectonized" zone on the left bank of the pre-1963 Vaiont Gorge, as mapped by SELLI & TREVISAN (1964) and identified as the outcrop of the pre-historic slide surface.

3) By matching the large part of the sliding surface exposed by the landslide in the upper levels of the slope and mapped recently by aerial Lidar (SUPERCHI, 2012).

4) By limiting the eastern margin of the sliding mass along the trace of the steep Col Tramontin fault (SUPERCHI, 2012).

5) By ensuring that the sliding surface is reasonably smooth in the downslope direction, although steps transverse to the direction of movement are accepted.

The reconstruction of the sliding surface was carried out using the three-dimensional slope stability program CLARA-W, which is designed to form a three-dimensional surface by interpolation between adjacent downslope cross-sections (HUNGR et alii, 1988). The input cross-sections were constructed at 200 m spacing, and drawn so as to satisfy Points 2), 3) and 5) above. Three of the sections were coincident with Rossi and Semenza Sections No. 2,5 and 10a, which are the best constrained by borehole information.

The resulting surface is shown in Fig. 1. The 1964 boreholes are posted with interpreted elevations of the main sliding surface. The shaded area in the top part of the slope indicates the zone where the reconstructed surface coincides approximately with the recent Lidar topography and thus shows the areas where the 1963 sliding surface is presently exposed.

The borehole information is shown to be approximately consistent with the reconstructed surface, except in Borehole 16, near the eastern flank of the landslide, where drilling information shows several alternative shear zones and the position of the main sliding surface is very uncertain. The surface outline of the slide also closely follows the outline determined from airphotos. The upper part of the reconstructed sliding surface coincides with the exposed area surveyed by Lidar. The volume of the landslide, based on this surface, is 294 million m^3. It is recognized that, in a landslide as large and complex as this, the sliding surface may consist of more than one discrete shear zone. In particular, the rupture surface is likely stepped in its eastern part and its reconstruction there is less certain.

However, given the great volume of material involved, departures from the assumed sliding surface shape are unlikely to have a major influence on the balance of forces. Other factors, especially the distribution of shear strength on the surface and the internal strength of the sliding body, are more important.

LIMIT EQUILIBRIUM ANALYSES
GEOTECHNICAL MODEL

The initial geotechnical model was derived from the conclusions of HENDRON & PATTON (1985) and uses the sliding surface described on Fig. 1. The model recognizes two types of shear strength, mobilized in different areas:

The main (western) part of the sliding surface is assumed to follow pre-sheared bedding planes or pre-existing shear zones, with an average friction angle of 12°, corresponding to a smooth, clay-filled discontinuity at residual strength. This assumption is based on the observation of the exposed southern parts of the surface, where shearing often clearly follows the rock structure.

However, the relationship between the bedding attitudes and the sliding surface is not simple. For example, the average bedding strikes measured by SUPERCHI (2012) in the eastern and western structural domains of the exposed surface are not exactly parallel with the average contours of the sliding surface. Therefore, the surface must be curved and/or stepped in these domains. The relationship between the bedding and the sliding surface is even more complex in the central structural domain, which exhibits complicated folding interference features and crushed zones. The blanket assignment of the 12° residual friction angle is therefore not unambiguous and will be discussed further.

The internal strength of the limestone rock mass was estimated using the HOEK-BROWN (1980) rock mass strength model. The rock mass strength envelope was derived by the software RocLab, Version 1 of RocScience, Ltd. and is based on empirical equations developed by E. Hoek and co-workers during the nineteen-nineties (HOEK et alii, 2002). The mean properties of the rock mass were determined using typical indices based on detailed field and laboratory work by SUPERCHI (2012): Uniaxial Compressive Strength of 50 MPa and an average Geological Strength Index (GSI) of 50. With a rock pressure corresponding to a depth of 250 m, these indices yield an equivalent cohesion of 1500 kPa and a friction angle of 34°. These values were considered as an upper limit of rock strength on surfaces perpendicular or oblique to the

53

bedding. There are reasons to consider that the cohesion value may be substantially less in some locations, as discussed below.

Rock structure has a very strong influence on the geotechnical model. The bedding structures daylight along the western margin of the landslide, which allows the blanket assignment of the weaker bedding-parallel strength in the western region. The distribution of shear strength is particularly complex in the eastern part of the sliding surface. Even though new geological observations and the discovery of the north-south trending Messalezza Syncline have complicated the picture, it is still apparent that the bedding planes plunge into the rock mass bordering the right flank of the landslide. This likely happens in step-like manner, as proposed by HENDRON & PATTON in Figs. 21 and 22 of their report. The existence of this phenomenon is supported by the multiplicity of sheared zones intersected by Boreholes 9 and 16. Also, the shape of the sliding surface near the eastern flank departs from the characteristic chair-shaped morphology of the central region. A near-vertical cliff, more than 100 m high, bounds the eastern margin of the slide, corresponding approximately with the trace of the Col Tramontin fault. The pre-failure displacement measurements reported by MÜLLER (1964 and 1968) indicated clockwise rotation of the slide mass, suggesting that the right (eastern) flank was constrained by an increased strength of the rupture surface in this area.

Based on the above arguments, the geotechnical model used the lower (bedding) shear strength for the greater, western part of the sliding surface, while the higher rock mass strength was used for that part of the surface extending from x=1500 m to the eastern margin.

Also, the internal strength of the slide was assumed to be the rock mass strength, in sections where internal deformation is required to make motion kinematically feasible.

The piezometric surface associated with the rupture surface of Fig. 1 was obtained by interpolation of the highest piezometric lines assumed for Sections 2, 5 and 10a by HENDRON & PATTON (1985). Guided by the limited water well level observations made prior to the landslide and by the record of landslide behaviour relative to precipitation, HENDRON & PATTON assumed that the piezometric surface was determined partly by the water level in the reservoir, but increased significantly due to heavy rainfall infiltration. The assumed surface exhibits artesian pressures along the reservoir shoreline, in a narrow band parallel with the landslide toe.

A standard toe submergence procedure of including the weight of the reservoir water above the sliding surface and adding a total horizontal hydrostatic thrust force was used in the analysis. The hydrostatic thrust force amounted to 1.1% of the slide weight and the corresponding increase in the Factors of Safety due to toe submergence was of the order of 4%.

TWO-DIMENSIONAL ANALYSIS

Three different 2D methods of limit equilibrium analysis were utilized in this case. The first one, Bishop's Simplified Method, with modifications due to FREDLUND
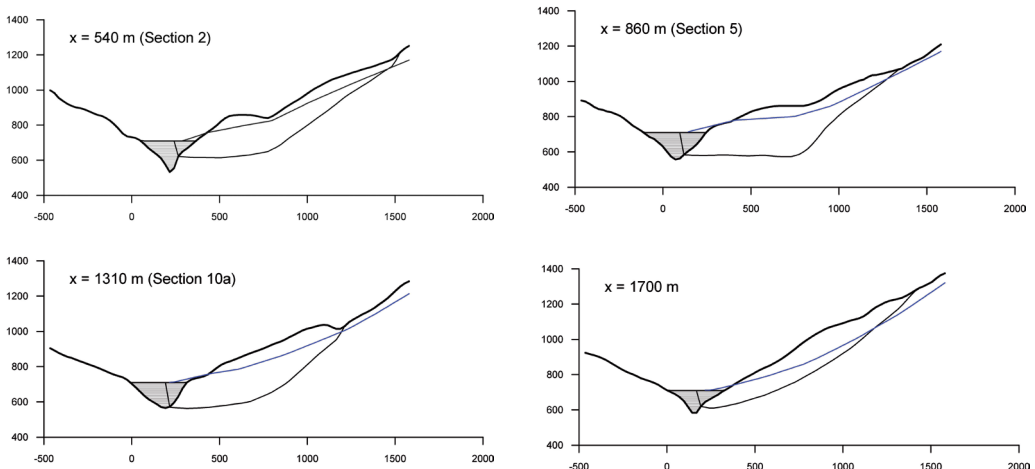
Fig. 2 - Cross-sections of the sliding surface, used in the 2D analyses

54

International Conference on Vajont - 1963-2013 - Thoughts and analyses after 50 years since the catastrophic landslide   Padua, Italy - 8-10 October 2013

& KRAHN (1977) to allow the use of non-rotational sliding surfaces, explicitly neglects the internal strength of the sliding body. Its advantage here is that a three-dimensional version is available, which permits searching for the critical direction of sliding. The Morgenstern-Price Method is a "rigorous method" in that it satisfies all equations of equilibrium and does include the influence of internal strength. However, the internal strength is not specified as a function of material properties, but is assigned by the solution algorithm so as to simultaneously satisfy the moment and force equilibrium (FREDLUND & KRAHN, 1977). There is also a 3D version of this method implemented in the program CLARA-W, but it cannot at present be optimized with respect to the direction of sliding. The third method used is the Sarma Method as programmed by HOEK (1997). The Sarma Method is also a rigorous method. It relies on an explicit assignment of strength on internal surfaces of the sliding body. In this, the method resembles the technique used by HENDRON & PATTON (1985).

Using the program CLARA-W, limit equilibrium analyses were first conducted on four cross-sections drawn in the downslope direction, as presented in Fig. 2. The first three of these sections coincide with the Rossi-Semenza sections mentioned previously. Their locations can be determined using the x-coordinates on Fig. 1. Sections 2 and 5 were also simplified in the form of blocks separated by vertical boundaries as shown in Fig. 3 and analysed using a Sarma program kindly provided to the author by Prof. E. HOEK and based on HOEK (1997).

Strength properties and piezometric levels were assigned as described in the previous section. For Sections 2, 5 and 10a, the shear strength of the sliding surface is based on $\phi=12°$ and zero cohesion, while the internal strength for the Sarma Method involves $\phi=34°$, with or without a cohesion of 1500 kPa. The additional section at x=1700 m, close to the eastern flank, was assigned a basal friction angle of 34° (no

cohesion). Sarma analyses were completed only for the first two sections. For the remaining two (10a and x=1700) the Sarma program did not converge. In any case, these sections are close to a circular shape, so are unlikely to benefit very strongly from mobilization of internal strength. Therefore, the Sarma Factor of Safety for these sections is likely similar to that of Morgenstern Price.

The results reported in Table 1 indicate that the influence of mobilized internal strength is not very great, unless the full value of internal cohesion is included. Without internal cohesion (although a high internal friction angle of 34° is used), the Sarma results exceed the Bishop Factors of Safety by 10-16% for the two chair-shaped Sections 2 and 5 and likely much less for the remaining sections. Only with fully-mobilized internal cohesion does the internal strength account for about 40% stability increase in Sections 2 and 5 and likely less in the remaining sections. The Morgenstern-Price Method predicts a much smaller influence of internal strength of less than 10% (Spencer's Method was also used and yielded very similar results). Because the non-rotational Cross-sections 2 and 5 represent only about one half if the slide volume, the overall effect of mobilized strength on the stability of the slide is likely in the range of 20-25% with cohesion and 5% without. This is significant, because loss of internal cohesion due to large-scale deformation during movement will lead to a significant reduction of the resisting forces, leading to brittle acceleration of the landslide.

Section	Bishop's Simplified	Morgenstern-Price	Sarma c=0	Sarma c=1500 kPa
#2, x=540	0.43	0.44	0.48	0.66
#5, x=860	0.60	0.66	0.70	0.86
#10a, x=1310	0.42	0.43	[1]	[1]
x=1700 (rock)	2.29	2.28	[2]	[2]

[1] No convergence [2] Circular section, not analysed

Tab. 1 - *Two-dimensional factors of safety for four representative cross-sections*
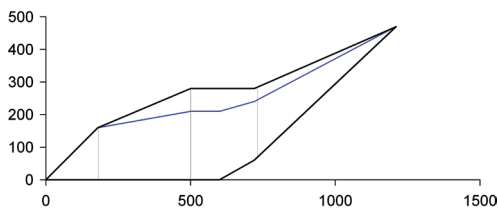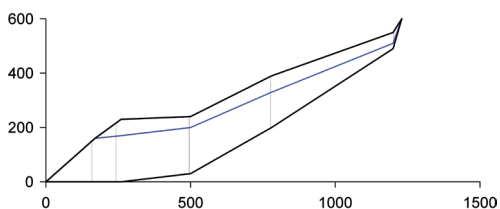
Fig. 3   *Cross-sections 2 and 5, represented as block assemblies for analysis using the Sarma Method*

All of the sections located within the part of the sliding surface that exposes bedding-parallel shears are highly unstable, even with full mobilization of internal strength. Only the section at x=1700 m, considered to lie within the constraining zone, has a much higher Factor of Safety, derived from the strength of the rock mass. The stability of the slide thus relies to a very large degree on the strength and spatial extent of the easterly constraining zone of rock mass, as was also concluded by HENDRON & PATTON (1985). It is possible that the presented geotechnical model exaggerates this phenomenon. A further discussion of this is provided below.

Basal friction angles that would be required for each section to be stable on its own would be 26°, 18°, 26.5° and 32° for Sections 2,5,10a and x=1700 respectively, using the Morgenstern-Price Method. These represent the maximum strength values that the sliding surface could possibly have had.

THREE-DIMENSIONAL ANALYSIS

A 3D model was assembled in CLARA-W, using the sliding surface shown in Fig. 1 and Fig. 4. The strength parameters, a piezometric surface and toe submergence are the same as used in the 2D analyses shown in Fig. 2. The assumed distribution of the two types of shear strength on a plan of the sliding surface is shown in Fig. 5

Condition	Bishop's Simplified	Bishop's Rotated 10°	Morgenstern-Price
No constraint, uniform strength	0.42	0.47	0.46
Constraint, φ=34°, c=1500 kPa	1.07	0.92	1.19
Constraint, φ=34°, c=0	0.60	0.62	0.67

Tab. 2 - Summary of the 3D LE analyses carried out with the reviewed geotechnical model, with bedding-parallel friction angle of 12° and a constraint placed as shown in Fig. 5
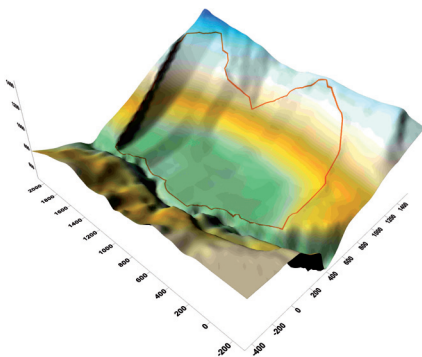
Fig. 4 - An isometric view of the assumed rupture surface (see also Fig. 1). Published slide outline shown

The strength of the constraining zone was considered both with and without a cohesion of 1500 kPa. Because large parts of the constraint are probably subject to tensile stresses, as considered by Hungr and Amann (2010), cohesion is likely to have been destroyed in a large proportion of the constraint surface. Thus, the c=0 model is considered more realistic.

The results of the 3D analyses are shown in Table 2. The analyses show that the constraint is essential in order to maintain marginal stability of the landslide, even if an allowance for increased resistance due to internal shear strength of the cross-sections is allowed for (up to a maximum of 25%, as discussed earlier). This finding is in accord with the conclusions of HENDRON & PATTON (1985). Cohesion within the constraint appears especially important and the slide could not be stable without it with the assumed strength parameters. A loss of cohesion within the constraint could reduce the overall resisting forces within the landslide by 50% and marginal stability could not be achieved.

The analysis provides some other conclusions. If there is cohesion within the constraint, a rotation of the direction in which the forces are resolved by 10° counter-clockwise from the negative-y-axis could reduce the Factor of Safety by more than 10%. But this effect is not observed without cohesion.

The high piezometric surface proposed by Hendron and Patton is necessary for instability. If the piezometric surface was reduced to the level of the reservoir, the minimum 3D Factor of Safety would be 1.10.
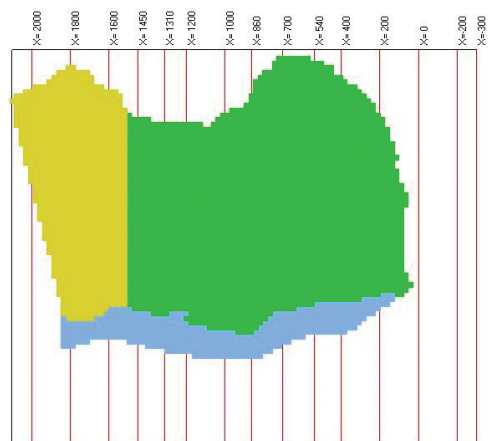
Fig. 5 - A plan of the sliding surface output from CLARA-W. The green area on the right is the part of the sliding surface following bedding-parallel shears. The yellow area on the left is the constraint, where rock mass shear strength is assumed to prevail

56

International Conference on Vajont - 1963-2013 - Thoughts and analyses after 50 years since the catastrophic landslide Padua, Italy - 8-10 October 2013

A further discussion of these results is provided in the Conclusions.

ANALYSIS OF MOTION
TWO-DIMENSIONAL DYNAMIC ANALYSIS

Dynamic analysis of landslide motion is not yet a routine procedure at present, although significant advances in the application of models have been made in recent years. Most current models are unsteady flow models based on an integrated ("shallow water") solution of the equations of motion (e.g. HUNGR *et alii*, 2005). However, such solutions cannot be applied to the Vaiont Slide, which is known to have moved by several hundreds of metres as a nearly solid block. Evidence of this is provided by the preserved stratigraphy around the margins of the deposit and on the surface (SUPERCHI, 2012).

The overall volume of the detached mass, as estimated by subtracting the assumed sliding surface of Fig. 1 from the pre-1963 ground surface is 294 million m³. The deposit volume, obtained by subtracting the sliding surface from the post-slide topography is 286 million m³. The latter number could be larger because the calculation was carried out only within the limits of the 3D stability model, as shown in Fig. 1. Certain material which ran into the valley upstream of the eastern boundary of the model is not accounted for. Also, there could be some difference between the pre-1963 topography and the recent Lidar-derived model. In any case, there is no evidence of substantial bulking of the deposit, which confirms the hypothesis of a nearly-intact sliding block

The dynamic analysis therefore utilized two experimental semi-flexible block models, which are currently under development at the University of British Columbia. The premise of the modelling is that the planar layout of the landslide mass remains essentially intact, like a semi-flexible blanket which is able to shear in the vertical direction, but remains coherent in plan. A similar model was used at Vaiont in two dimensions by ROMERO & MOLINA (1974).

A two-dimensional motion analysis was first carried out using a modification of the 2D shallow flow model DAN-W (HUNGR, 1995). The modification involved forcing the assembly of reference blocks to remain coherent in the downslope direction. In order to achieve this, instead of solving the equation of motion separately for each element, the driving forces and resisting forces for all elements, without the pressure term, were each summed into a single resultant force in each time step and the net force was used to accelerate the flexible body down the slope. Fig. 6b shows the resulting analysis, compared with the actual cross-section before and after the slide, as obtained from the digital terrain models as shown in Fig. 6a. The analysis assumed that the friction angle on the base of the slide was 23°, combined with a constant pore-pressure coefficient ru (ratio of pore-pressure to total vertical stress) which corresponds to the high piezometric pressure as assumed in previous analyses. The analysis shows a fair agreement with the observation. The slide is displaced by about 270 m, having reached a maximum velocity of 14 m/s.

The basal friction angle of 23°, back-analysed by the dynamic model is substantially higher than the 12° used in the stability analyses. One reason for this is that the dynamic calculations neglect internal strength of the sliding body. This was seen to be able to increase the stability of this cross-section by 11% to 40%, depending on whether cohesion is fully active (as seen in Table 1 by comparing the Sarma and Bishop results). The second reason is that, according to the 3D analyses,
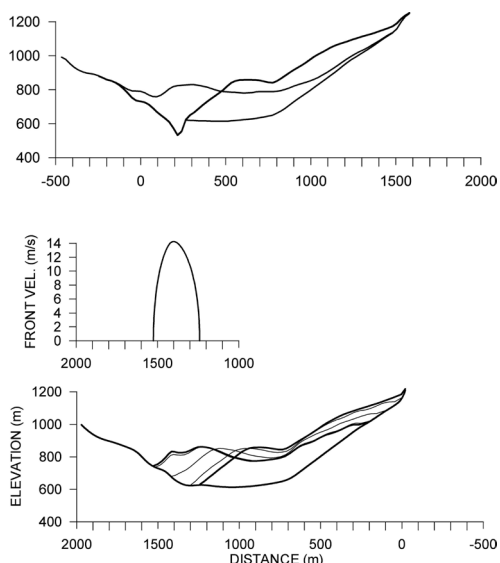
Fig. 6 a) Cross-section 2 (x=540 m), before and after the 1963 slide. b) Cross-section 2 before and after the slide, analysed with the 2D flexible block model, with ϕ=23° and an ru of 0.4. The thin lines are profiles at 10 second intervals. The inset shows the velocity profile of the front

57

Section 2 could not be stable without contribution from the 3D effects. A third possible explanation, however is that the 12° bulk friction of the western lobe of the slide is, perhaps an underestimation.

Internal strength acts in the first vertical curve of the chair-shaped profile, as pointed out previously by MENCL (1966) and others. However, an even greater influence of internal strength is likely to play a role during motion, as the landslide front impacts the right side of the Vaiont gorge and is forced upward. This impact was so powerful that a part of the right bank was, in fact, entrained by the slide and thrust upward (HENDRON & PATTON, 1985).

3D DYNAMICS OF A SEMI-FLEXIBLE BLOCK

The above-described method of dynamic analysis of a flexible block was extended into three dimensions. The model was configured in the same manner as the 3D Limit Equilibrium analysis, by simulating the landslide mass by an assembly of over 2000 vertical columns. The driving force on each column was determined as the downslope component of its weight. The forces from all columns were then summed into one driving force resultant. In the same way, the resisting forces on the column bases were determined by assuming zero frictional stresses on vertical column boudaries and taking into account the friction of the sliding surface and the piezometric pressure prevalent at the moment of failure. Again, these forces were combined into a single resultant. The translatory motion of the slide was determined in time steps, by determining a constant acceleration as the ratio of the net resultant force and the mass of the sliding body. Rotation of the sliding block around the vertical axis was then determined from the torque exerted by the driving and resisting resultants and dividing by the moment of inertia of the sliding mass. The accelerations were integrated to obtain both translatory and rotational velocities and displacements and these were distributed to the individual columns, depending on their radial distance from the centre of rotation.
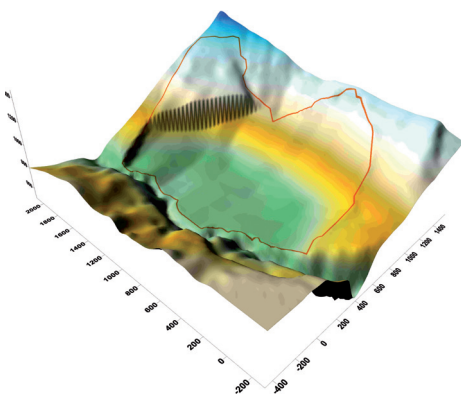
The initial analysis was made using the same strength properties of the sliding surface as used for the LE analysis. The larger, western part of the surface was given a friction angle of 12° and a constraint, at x>1500 m was given the friction angle of the rock mass, 34°. The slide was seen to rotate strongly clockwise and overshot the observed displacement on the western side by several hundred metres. As shown in Fig. 8, a better correspondence with observations was obtained by increasing the bedding-parallel strength to 23°. This result compares favourably with the above-described 2D analysis of Section 2 and can be explained using the same arguments.

Fig. 9 shows perspective views of the slide before failure, after 1963 as surveyed by Lidar and a comparison with the 3D analysis result. The model shows unrealistic distortion of the debris surface at the location of the Vailont Gorge, because no attempt was made to simulate the filling of the gorge.

The 3D dynamic analysis is reasonable qualitatively, but it again shows the need to better account for the internal strength of the sliding body. It also seems to exaggerate the degree of rotation of the sliding mass. This indicates that the initial geotechnical model may be underestimating the shear strength of the western part of the sliding surface.

Fig. 7 - Truncated" sliding surface of the Stage 1 failure used in the analyses summarized in Tab. 3
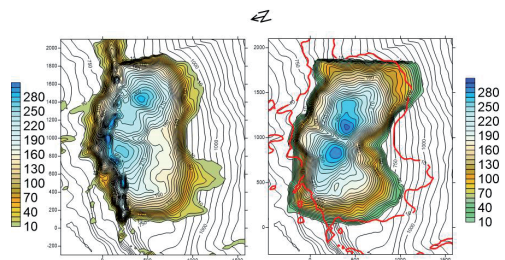
Fig. 8 - Isopachs of the Vaiont deposit. a) as obtained from the Lidar survey. b) Calculated using the flexible block model

58

International Conference on Vajont - 1963-2013 - Thoughts and analyses after 50 years since the catastrophic landslide Padua, Italy - 8-10 October 2013
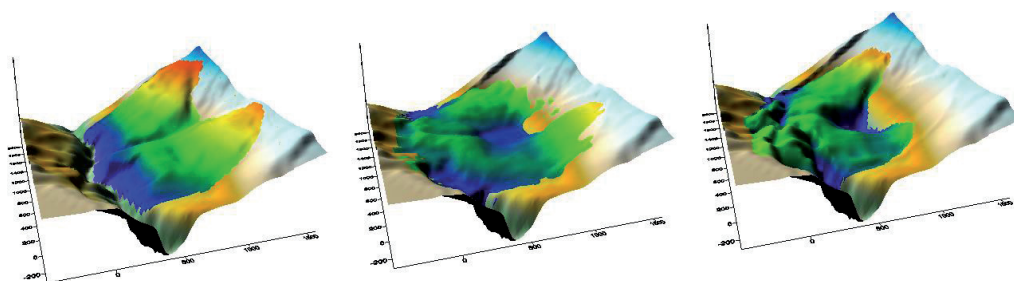
Fig. 9 - Isometric views of the Vaiont slide. a) before the slide, b) after the slide as surveyed by Lidar, c) Result of the flexible block dynamic calculation

TWO-STAGE FAILURE

The concentration of strength near the right (east) flank gives the landslide a tendency to rotate clockwise around a vertical axis. This trend is confirmed by pre-failure displacement observations (Müller, 1964 and 1968), as well as by the behaviour of the 3D dynamic model. During the pre-failure deformation period, this tendency to rotate must have generated high shear stresses on downslope-oriented vertical planes near the right margin of the slide, associated with tensile streses in the east-west direction. Such stress conditions were analysed by Hungr & Amman (2011), with examples of asymmetric, laterally constrained planar and wedge slides. A tendency of the tensile stress to destroy cohesion within the rock mass forming the constraint was noted.

The highest value of tensile stresses within the rock
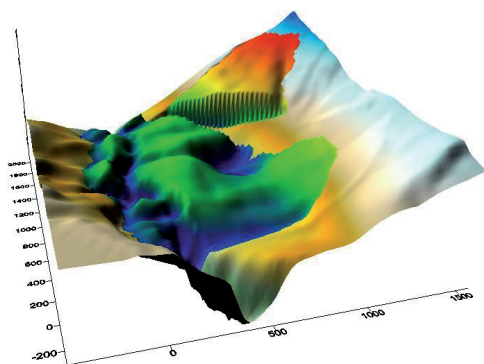
Fig. 10 - Stage 1 failure runout, as analysed using the 3D flexible block model. The remnant block remains in its original position

Condition	Bishop's Simplified	Bishop's Rotated 10°	Morgenstern-Price
No constraint, uniform strength	0.42	0.47	0.46
Constraint, ϕ=34°, c=1500 kPa	1.07	0.92	1.19
Constraint, ϕ=34°, c=0	0.60	0.62	0.67

Tab. 3 - Summary of the 3D LE analyses representing the first stage of a two-stage failure (see Fig. 7 and Fig. 10)

mass would be associated with diagonal tension, acting at a direction oriented 45° to the planes of maximum shear, oblique to the direction of sliding. As proposed by Superchi (2012), the sliding mass may have separated in course of failure along an oblique plane perpendicular to this tensile stress field. A corresponding "truncated" rupture surface was constructed as shown in Fig. 7. The volume of the first stage failure is approximately 280 million cubic metres. A remnant volume of approximately 40 million m³ is left in place. The analysis used the same strength and piezometric properties as used for the whole landslide.

The 3D LE analyses are summarized in Table 3, and can be compared with Lines 2 and 3 of Table 2. This comparison indicates that the truncated volume is about 20% less stable than the full volume of the slide. This confirms that the two-stage failure hypothesis (Superchi, 2011 and Superchi et alii, 2010) is very plausible.

The motion of the truncated Stage 1 landslide was simulated using the flexible block model as shown in Fig. 10. The block is predicted to shift downslope and rotate clockwise, exposing a high cliff in the north-east corner and removing support from the 40 million m³ remnant block. Although this second failure stage was not modelled, in all likelihood, the remnant block would fail almost simultaneously and follow the main mass to form the final deposit, as described by Superchi (2012).

LANDSLIDE WAVE

A variety of closed form and numerical techniques exist to simulate the water waves generated by the displacement of reservoir water by landslides (e.g. Slingerland & Voight, 1978, Heller et alii, 2009). The Vaiont case is not easily adaptable to routine analysis, because the volume of the water is much smaller than the volume of the landslide masses displacing it.

59
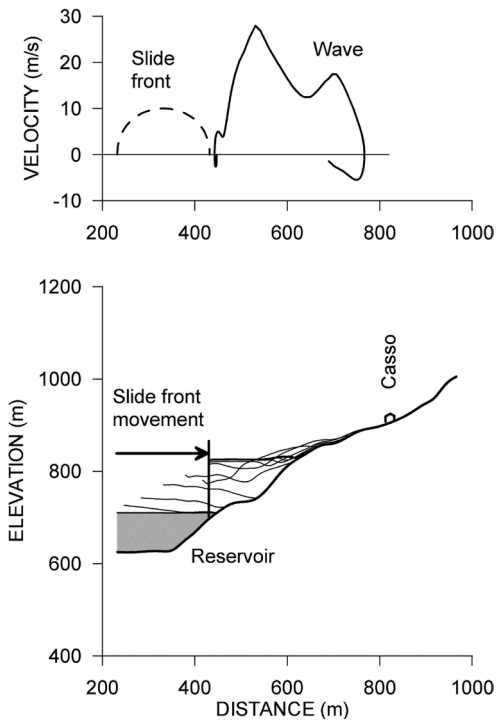
Fig. 11 - *Prediction of the displacement wave, assuming a peak landslide velocity of 10 m/s and a total displacement of 200m. The thin lines show the wave profile at 5 sec. intervals*

Fig. 12   *Prediction of the displacement wave, assuming a peak landslide velocity of 20 m/s and a total displacement of 200m. The thin lines show the wave profile at 2.5 sec. intervals*

Also, the moving landslide forces the reservoir volume against a steep and uneven opposing slope.

A simplified analysis was carried out by adapting an existing two-dimensional depth-integrated unsteady flow model DAN-W (HUNGR, 1995). In its standard configuration, the model accepts a volume of fluid and allows it to flow in directions dictated by the inclination of the pressure potential surface. In the modification developed for this analysis the left boundary of the model was assumed to be a vertical wall equal to the depth of the reservoir at the location of the toe of the sliding surface of the Vaiont Slide (Fig. 11). This vertical boundary was then forced to move towards the opposite shoreline at a prescribed rate of movement, pushing the water in front of it. Turbulent water flow was assumed.

The prescribed movement rate assumed a parabolic velocity distribution in time, by an equation:

$$V = AT^2 + BT \qquad (Eq. 1)$$

Integrating Equation [1], one obtains a formula that permits dimensioning the constants a and b in such a way as to obtain a user-prescribed maximum ve-

locity and total displacement and an equation tracing the displacement of the problem boundary in time. The resulting prescribed landslide velocity profile is shown by the dashed line in the upper part of Fig. 11 for a maximum velocity of 10 m/s. The maximum displacement was taken as 200 m to allow for volume of landslide debris lost in filling the Vaiont gorge. The slide duration is 30 seconds. As can be seen by the full line in the upper part of Fig. 11, the front of the wave advances about 3 times faster than the motion of the landslide, due to the geometric run-up magnification. The given input, i.e. maximum velocity of 10 m/s produces good agreement with the observed wave runup, and the height of overtopping of the Vaiont Dam.

The same analysis is repeated in Fig. 12 for a maximum slide velocity of 20 m/s. The predicted runup is extreme and unrealistic in this case.

60

International Conference on Vajont - 1963-2013 - Thoughts and analyses after 50 years since the catastrophic landslide   Padua, Italy - 8-10 October 2013

DISCUSSION AND CONCLUSIONS

The relatively simple models presented above are certainly not an exact representation of the complex phenomenon that is the Vaiont Slide. They do, however, permit some useful conclusions.

The underlying cause of the landslide was the widespread presence of weak, pre-sheared bedding planes in the slope. High piezometric pressures, considerably above the level of the reservoir, were also a necessary condition.

The present analysis confirms the hypothesis of HENDRON & PATTON (1985), that internal strength of the limestone rock mass plays an important role both in increasing the sliding resistance of cross-sections characterized by listric compound shape and in providing a 3D lateral constraint near the right (eastern) margin of the slide. The importance of internal strength depends strongly on the degree in which the large cohesive component is preserved.

The initial model, studied in this article, assumes that the bedding-parallel shear strength is very low (ϕ=12°) and that the internal cohesion is fully mobilized. An alternative condition could be that the bulk bedding-parallel shear strength is somewhat higher (say, 23°), while the internal rock mass cohesion is somewhat reduced. This alternative hypothesis would be in agreement with the observation that the sliding surface does not generally follow the precise orientation of bedding, especially in the central portion of the sliding surface and that the limestone layers overlying the rupture surface showed much disturbance and crushing, before 1963.

It is certainly surprising that the great deficit of resisting force in the western part of the slide that, as implicit in the model, could be transferred to the lateral constraint, without stresses. The present analysis supports this hypothesis.

The analysis of motion carried out during this study in two and three dimensions also suggests that the assumed 12° strength of the bedding-parallel surfaces may be too low. However, this analysis is handicapped somewhat by being unable to account for the internal strength of the sliding body. This effect is likely to be important in the later stages of motion, where the sliding mass contacts the opposite slope of the Gorge.

Another uncertainty connected with the dynamic analysis is the pore water pressure. Some authors, including HENDRON & PATTON (1985) hypothesized a strength loss due to frictional heating effects on the sliding surface. On the other hand, the sliding surface is known not to be perfectly thin and smooth. The prehistoric slide created a sizeable zone of crushed rock in the vicinity of the sliding surface. Dilatancy connected with such failure behaviour would negate any pore-pressure increases that could conceivably result from heating. In any event, the dynamic behaviour of the slide is strongly controlled by the process of internal cohesion strength loss and pore-pressure variation due to dilatancy, so that a frictional heating model cannot be reasonably proven or constrained.

An analysis of the displacement wave, carried out using an original model, concludes that the maximum slide velocity was of the order of 10 m/s. Given the geometry of the Vaiont reservoir and the steep slopes of the right bank, previously-reported velocities of the order of several tens of m/s would produce totally unrealistic wave runup.

ACKNOWLEDGMENTS

REFERENCES

FREDLUND D.G. & KRAHN J. (1977) - *Comparison of slope stability methods of analysis.* Canadian Geotechnical Journal, **14:** 429-439.

HELLER V., HAGER W.H. & MINOR H.E. (2009) - *Landslide generated impulse waves in reservoirs: basics and computation.* Mitteilungen 211, Versuchsanstalt für Wasserbau, Hydrologie un Glaziologie, R. Boes, Hrsg., ETH Zürich.

HENDRON A.J. & PATTON F.D. (1985) - *The Vaiont Slide, a geotechnical analysis based on new geologic observations of the failure surface.* Technical Report GL- 85-5, U.S. Army Engineer Waterways Experiment Station, Vicksburg, MS. I, II.

HOEK E. (1997) - *General 2-dimensional slope stability analysis.* In: BROWN E.T. (ED.). *Analytical and Computational Methods in Engineering Rock Mechanics.* 95-128, Allen and Unwin, London.

HOEK E. & BROWN E.T. (1980) - *Underground excavations in rock.* Institute of Mining and Metallurgy. Stephen Austin and Sons Ltd., Hertford, London, 527 pp.

HOEK E., CARANZA-TORRES C.T. & CORCUM B. (2002) - *Hoek–Brown failure criterion-2002 edition.* In: BAWDEN H.R.W., CURRAN J. & TELSENICKI M. (EDS.) - Proceedings of the North American Rock Mechanics Society (NARMS-TAC 2002). Mining Innovation and Technology, Toronto: 267-273.

HUNGR O., SALGADO F.M. & BYRNE P.M. (1989) - *Evaluation of a three-dimensional method of slope stability analysis.* Canadian Geotechnical Journal, **27**: 679-686.

HUTCHINSON J.N. (1988) - *General report: morphological and geotechnical parameters of landslides in relation to geology and hydrogeology.* In: Proceedings of the 5th International Symposium on Landslides, Lausanne, **1**: 3-35.

HUNGR O., COROMINAS J. & EBERHARDT E. (2005) - *State of the Art Paper #4, Estimating landslide motion mechanism, travel distance and velocity.* In: HUNGR O., FELL R., COUTURE R. & EBERHARDT E. (EDS.). *Landslide risk management.* Proceedings, Vancouver Conference. Taylor and Francis Group, London.

HUNGR O. & AMANN F. (2011) - *Limit equilibrium of asymmetric, laterally-constrained rockslides.* International Journal of Rock Mechanics and Mining Sciences, **48**: 748-758.

MENCL V. (1966) - *Mechanics of landslides with non-circular slip surfaces with special reference to the Vaiont slide.* Géotechnique, **XVI** (4): 329-337.

MÜLLER L. (1964) - *The Rock slide in the Vaiont valley.* Rock Mechanics andEngineering Geology, **2**: 148-212.

MÜLLER L. (1968) - *New considerations on the Vaiont slide.* Rock Mechanics and Engineering Geology, **6**: 1-91.

ROMERO S.U. & MOLINA R. (1974) - *Kinematic aspects of the Vaiont Slide.* Proceedings of the 3rd Congress ISRM, Denver, Colorado, **2**: 865-870.

SELLI R., TREVISAN L., CARLONI C.G., MAZZANTI R. & CIABATTI M. (1964) - *La Frana delVajont.* Giornale di Geologia, serie **20**, **XXXII** (I): 1-154.

SEMENZA E. & GHIROTTI M. (2000) - *History of the 1963 Vaiont slide: the importance of geological factors.* Bulletin of Engineering Geology and the Environment, **59**: 87-97.

SITAR N.M., MACLAUGHLIN M.M. & DOOLIN D.M. (2005) - *Influence of kinematics on landslide mobility and failure mode.* Journal of Geotechnical and Geoenvironmental Engineering ASCE, **131** (6): 716-728.

SLINGERLAND R.L. & VOIGHT B. (1979) - *Occurrences, properties, and predictive models of landslide-generated impulse waves.* In: VOIGHT B. (ED.). *Developments in geotechnical engineering, rockslides and avalanches*, **2**: 317-397, Elsevier, Amsterdam.

SUPERCHI L., FLORIS M., GHIROTTI M., GENEVOIS R. & STEAD D. (2010) - *Implementation of a geodatabase of published and unpublished data on the catastrophic Vajont landslide.* Natural Hazards and Earth System Sciences, **10:** 865-873.

SUPERCHI L. (2011) - *The Vajont rockslide: new techniques and traditional methods to re-evaluate the catastrophic event.* Ph.D. Thesis, University of Padova, 188 pp.

VOIGHT B. & FAUST C. (1982) - *Frictional heat and strength loss in same rapid slides.* Géotechnique, **32** (1): 43-54.

62

International Conference on Vajont - 1963-2013 - Thoughts and analyses after 50 years since the catastrophic landslide   Padua, Italy - 8-10 October 2013